Chapter 02: Selection of Glass forming Fe-alloys based on empirical correlation

2.1 Introduction

The widespread intention for research on metallic glasses is driven by basically two interests. The first is related to the fundamental interest of knowing the structure and properties of disordered materials and the second refers to their potential in structural and functional applications. Metallic glasses (MGs) have lack of long-range translational order. They can only be understood in terms of short-range order (SRO) and medium-range order (MRO)[125]. The lack of long-range translational order gives rise to diffuse halos in diffraction patterns unlike that of translationally ordered solids displaying sharp Braggs peaks. As a consequence of this, the structural characterization of MGs and bulk metallic glasses (BMGs) poses different kinds of challenges. The purpose of this chapter is to discuss the factors that encourage the glass-forming ability (GFA) and to evolve an alloy's selection criteria for MGs. Many authors have proposed empirical models to assess the glass-forming ability (GFA) of metallic systems. Various models of GFA are discussed in reviews as well as in monographs[4], [20], [126]. In a multi-component system, a confusion principle has been advocated by Greer in the year 1993 for GFA[18]. It is said in this paper that the GFA of BMGs tends to increase with the number of constituent elements. Inoue has proposed three glass-forming criteria[24]. They refer to (i) the multi-component systems consisting of more than three elements, (ii) the atomic size ratio must be above 12% between main and constituent elements, and (iii) the heat of mixing among constituent elements should be negative. Alloys satisfying these empirical rules have been found to display atomic clusters in the liquid state promoting glass formation[126]. It was noticed that the GFA of any system involves two aspects. They relate to (i) the stability of liquid structure, and (ii) the resistance to crystallization. The former refers to the geometry of clusters and the latter pertains to the kinetic factors[20]. Bernal [21] advocated the glass-forming tendency of the metals based on the dense random packing (DRP) of the hard-sphere for a single-component system in the liquid state. The combination of constituent elements in a multi-component system having differences in radii as well as high negative heat of mixing[24] was seen to yield efficient packing of clusters (ECP)[22] thereby increasing the density of random packing of atoms in the super-cooled liquid state. Egami and Waseda [23] proposed the atomic volume strain criterion to predict GFA in binary alloys produced by the rapid solidification (RSP) technique. According to them, a minimum solute concentration is required to produce critical strain for the destabilization of the crystalline phases.

The density difference between the structurally relaxed and fully glassy state is about 0.11-0.15%. Thus small density difference between them suggests the glassy alloys contain dense randomly packed clusters [24]. Bota et al. [25] developed a new criterion to predict GFA based on electronegativity difference. They conclude that small differences in electronegativity tend to the formation of solid solutions otherwise stoichiometric compounds will form. Some researchers[26]–[29] have proposed simple parameters and tried to correlate them with GFA. These parameters are the kinetics process, nucleation growth rate, and crystal growth rate[30]. The GFA of metallic glasses is kinetically related to the viscosity of the liquid alloys[31]. Viscosity changes to temperature, known as fragility and it occurs around glass transition temperature (T_g) [32]. The concept of fragility was first proposed by Angell[127]. The fragility parameter (m) is inversely correlated to critical thickness (D_c) and directly correlated to the critical cooling rate (R_c)[33]. Turnbull [27] proposed reduced glass transition temperature ($T_{rg}=T_g/T_l$) with T_l as the temperature of the melt. There is no relation between the melt between the glass forming criteria of Inoue with Turnbull, Li, and Lu[19], [30]. I believe that all of these will be significant only when they get correlated with the nature of geometrical clusters. However, it is not an easy task. The work of Mircale[29] can be considered as a unique important step in this direction. Laws et al. [22] proposed the most efficient cluster packing (ECP) model for metallic glasses. Azad et al. [128] have given a Venn diagram for evolving criteria for metallic glass formation in terms of three parameters. These are (i) electron to atom ratio (e/a), (ii) Volume ratio (V_R), and (iii) radius ratio (R_R). In addition to these, they have also invoked the Fermi wave vector (K_F) and Pseudo Brillouin zone (PBZ) interactions in stabilizing the unique composition of the alloy.

2.2 Present Work

This work is based on alloy selection criteria that were proposed by Azad et al.[128]. I have chosen ~1000 compositions of MGs of various systems from literature. The data were analyzed to arrive at separate Venn diagrams for Fe-, Cu-, Zr-, Ti-, La-, Mg-, Co-, Al-, Ni-, and Pd-based systems respectively. We have also investigated K_F and PBZ interaction concepts for aforesaid systems is also considered. This chapter also discusses the importance of large unit cell-based intermetallic that is formed in similar alloy compositions akin to those of metallic glasses. This will be supported based on the diffraction analysis of metallic glasses from literature after their controlled crystallization. It is believed that such a correlation and models given by other researchers[19], [20], [26], [29], [30], [126] will improve understanding of the selection criteria of metallic glasses. Table 2.1 shows the type of system in terms of major

Table 2. 1: Type of metallic glasses based on different system

Systems	No. of Alloys	No. of Representative alloys
Fe	251	90
Cu	157	33
Zr	136	34
Ti	128	42
La	58	15
Mg	54	22
Co	52	15
Al	51	25
Ni	34	14
Pd	29	13

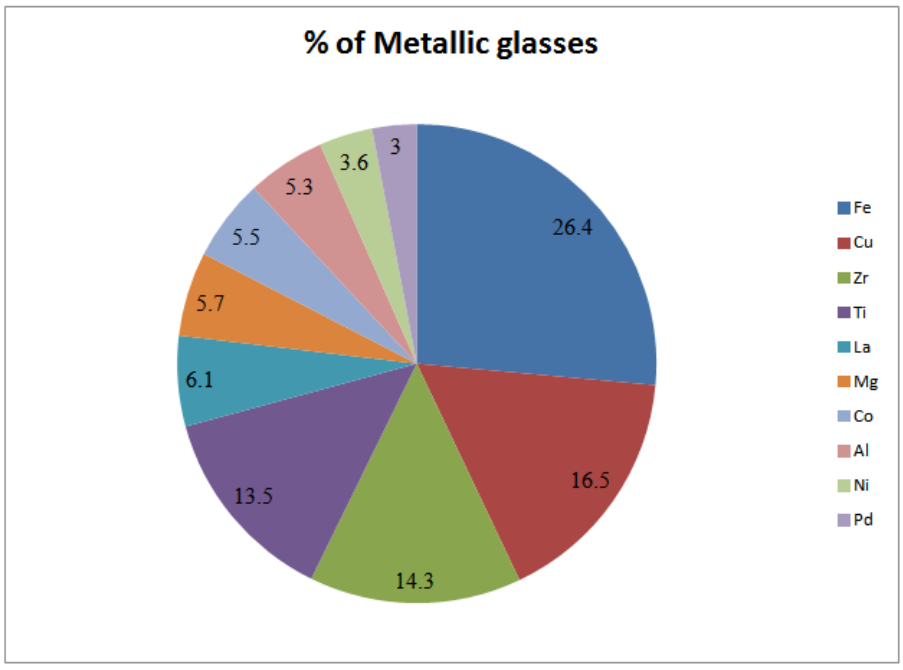

Fig. 2. 1: A pie-chart graph representing the number of metallic glasses (in %) based on a different system

alloying elements, number of alloys, and the total number of their representative alloys. Fig.2.1 represents a pie-chart graph that indicates the number of metallic glasses (in %) compositions based on alloy systems considered here.

2.3 Computation of glass-forming parameters (e/a, V_R, R_R, and K_F)

The electron-to-atom (e/a) ratio scale for structural stabilization and largest stability is a simple and promising criterion for searching for high glass-forming ability in a given system. The e/a parameter is especially favourable for the multi-component system. The e/a value has been estimated by different investigators. For example, the e/a value of Zr has been taken at 1.5 followed by Wang et al. and Pettifor [129]. Haussler [130] and Dong et al.[131] suggested alloy compositions of MGs having e/a value 1.8 are referred to as ideal glasses and seem to get stabilized by the Fermi-sphere and the Brillouin zone boundary interaction. The computation of the e/a value is really complicated due to sp-d hybridization effects, especially in transition metals[129]. For the computation of the e/a ratio, I have taken the valence states of various atoms from the work of Mott and Jones [132]. It has been observed that the dual nature of valency, depending on their roles (i.e., solvent or solute)[128].Those elements whose valency is not specified are taken from Pauling[133]. The valency of various elements of BMGs composition are given in Table 2.2.

Table 2. 2: State of Valence(s) of various Elements

Elements	Valence	Elements	Valence	Elements	Valence	Elements	Valence
Fe	+1(solvent) -2(solute)	Ni	0(solute) +1(solvent)	Co	-1(solute) +1(solvent)	Tb	+3.5
Li	+1	V	+5	Ga	+3.56	Dy	+3
Na	+1	Nb	+5	Si	+4	Ir	+6
Be	+2	Ta	+5	Pr	+3	Pd	+6
Mg	+2	C	+4	Nd	+3	Pt	+6
Ca	+2	Cr	-4	Eu	+3	Cu	+1
Sn	+2	Mo	+6	Hf	+4	Ag	+5.56
Ba	+2	W	+6	Zn	+4.56	Au	+4.56
Al	+3	Mn	-3	Ti	+4	S	+2
B	+3	Ge	+6	Gd	+3	Ce	+3.2
Y	+3	Pb	+2.56	Yb	+2	Er	+3
La	+3	P	+3	Ho	+3	Tm	+3

The minimum in the density of states when the Fermi surface is close. This is taken as a stabilizing criterion. This is numerically calculated by $2k_F = G$. Where k_F is the radius of the Fermi Wave vector, G is the diffraction peak that remains invariant for glass after its controlled crystallization.

For the calculation of k_F, the following expressions are used

$$k_F \text{ (Fermi vector) } (A^{o-1}) = \frac{\sqrt{2mE}}{\hbar}$$

$$\text{Fermi energy (E) (ev)} = 36.1(n_0/\Omega_0)^{2/3}$$

Where, n_o= e/a, and Ω_o= Average compositional volume per atom

I have considered two basic important parameters G_1 and G_2 and report their values based on the experimental observations of X-ray diffractions of MGs under different processing conditions from literature. These are referring to:

(i). G_1=reciprocal distance ($Å^{-1}$) of the first diffuse intensity maxima of the glass.

(ii) G_2=reciprocal distance ($Å^{-1}$) of the first intense peak around G_1 on the crystallization of the bulk metallic glasses.

Atomic size ratio (R_R) is another factor that is commonly invoked to account for phase stability and composition rule. It is defined as the ratio of the largest to smallest atom in the alloy system. The purpose of this work is to investigate the correlation between the atomic size ratio of the constituent elements and GFA for both metal-metal and metal-metalloid systems. The size factor plays a dominant role in determining the composition limit for glass formation. For the computation of size ratio, the radii of various elements present in MGs compositions have been taken from the website[134] and listed in Table 3 by considering the atoms are hard spheres.

$$\textbf{Radius ratio } (R_R) = R_{\text{largest atom}} / R_{\text{smallest atom}}$$

Another parameter considered was volume ratio (V_R), which is defined as the ratio of the average volume per atom of the alloy to the volume of the largest atom in the alloy system. This parameter is compositional dependent, unlike R_R. I have listed out MG composition along with relevant references and values of K_F, e/a, R_R, and V_R in Annexure-I.

$$\textbf{Volume ratio } (V_R) = V_{\text{avg. vol. per atom}} / V_{\text{largest atom}}$$

Table 2. 3: Value of atomic radius in (A^o) of various elements

Elements	Atomic radius	Elements	Atomic radius	Elements	Atomic radius
Fe	1.24	V	1.31	Pr	1.65
Ni	1.42	Nb	1.42	Nd	1.64
Co	1.25	Ta	1.43	Cd	1.56
Be	1.13	C	0.77	Hf	1.57
Mg	1.60	Cr	1.24	Zn	1.39
Ca	1.97	Mo	1.36	Ti	1.46
Sn	1.62	W	1.36	Gd	1.80

Tb	1.78	Mn	1.35	In	1.93
Al	1.43	Ge	2.11	Ho	1.75
B	0.82	Pb	1.75	Dy	1.77
Y	1.80	P	1.06	Sm	1.81
La	1.87	Ga	1.39	Pd	1.37
Zr	1.60	Si	1.15	Pt	1.391
Cu	1.27	Ce	1.82	S	1.0
Ag	1.44	Er	1.75		
Au	1.66	Th	2.40		

2.4. The e/a, V_R, and R_R criteria for BMGs

Based on the number of compositions based on various systems like Fe, Cu, Zr, Ti, La, Mg, Co, Al, Ni and Pd, e/a, V_R, R_R and K_F for these alloy compositions are calculated. Table 1-10 which are added in Annexure-I, show results of 90 Fe-based, 33 Cu-based, 34 Zr-based, 42 Ti-based, 15 La-based, 22 Mg-based, 15 Co-based, 25 Al-based, 14 Ni-based and 13 Pd-based representative alloy systems respectively. The numbering of alloys is indicated in column 1. The variations in compositions for a given alloy system are indicated in column 2. It was noted that all the metallic glass compositions satisfy at least one of the following criteria except alloy numbers 215 and 896 in Fe- and Co-based systems respectively. The value of the three parameters is out of range for these two alloys. In the Fe-based system, they relate to e/a values lying between 1 and 2, V_R values between 0.5 and 0.9 and R_R in the range of 1.5-2. One can understand their relative importance by referring to the Venn diagram. The Venn diagram with the help of the above three parameters (e/a, R_R, and V_R) for Fe-based systems is shown in Fig.2.2 (a). It can be noted from this figure that 89 systems fulfil at least one of the criteria mentioned above. Out of these, 84 systems confirmed to follow e/a ratio criterion, 58 systems follow V_R criteria, 72 systems follow above radius ratio R_R criteria and 49 alloy systems fall in the intersection regions of the three criteria. One may see that R_R criteria is independent of composition so its value is fixed for a given alloy system while e/a and V_R are dependent on composition. For a given alloy system, the values of e/a, and V_R lie in a range due to dependency of composition. Similarly, I have computed the aforementioned three parameters for Cu-, Zr-, Ti-, La-, Mg-, Co-, Al-, Ni-, and Pd-based system and their values are listed in Table 2.4. The nature of the fulfilment of these criteria through Venn diagrams is shown in Figs. 2.2, 2.3, and 2.4 with major alloying elements depicted in the captions.

From the above Venn diagrams, it was observed that those alloys that are lying in the intersection of three parameters have better GFA for MG formation. Out of ~1000 alloy systems, there are a total of 303 representative alloys which are investigated by us. Among these representative alloys the alloy numbers 269, 236, and 254 independently follow e/a, V_R, and R_R criteria respectively. Table 2.5 gives the numbers of alloy systems falling in the intersection regions of two or three different criteria in the above Venn diagrams. In Fe-based metallic glasses, better GFA may be expected.

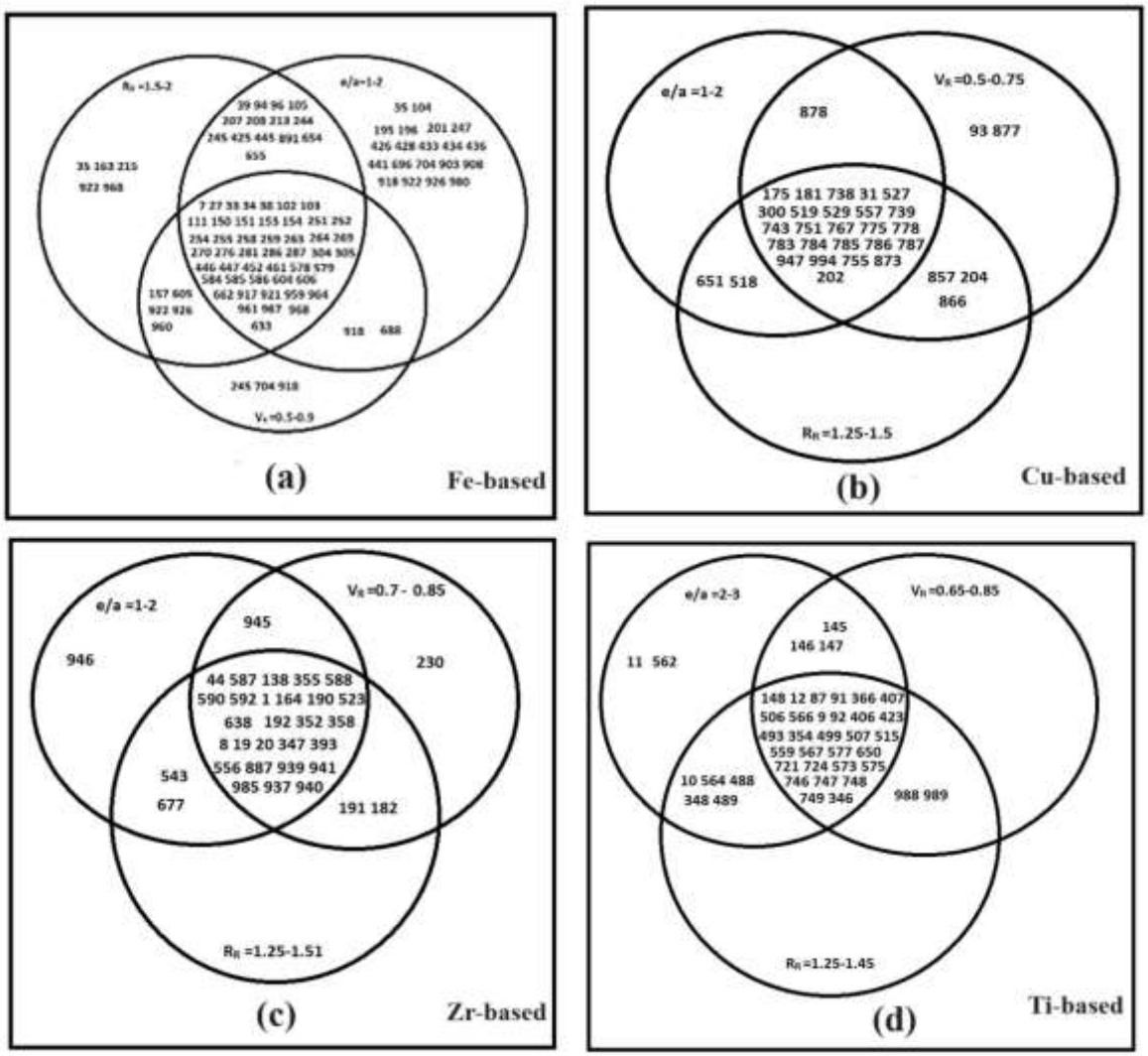

Fig. 2. 2: Venn diagram model (a) Fe-base system, (b) Cu-based system, (c) Zr-based system and (d) Ti-based system.

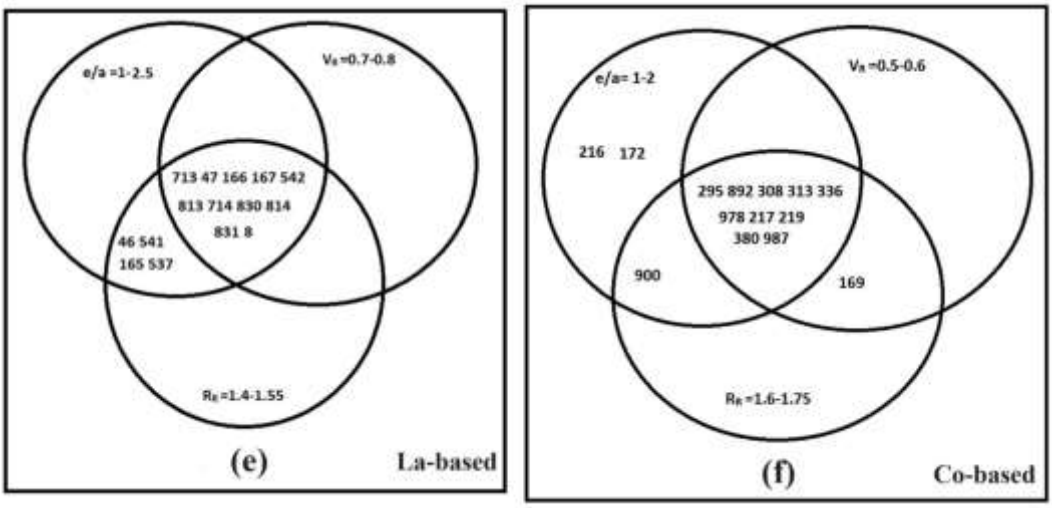

Fig. 2. 3: Venn diagram model for (e) La-based system, (f) Co-based system

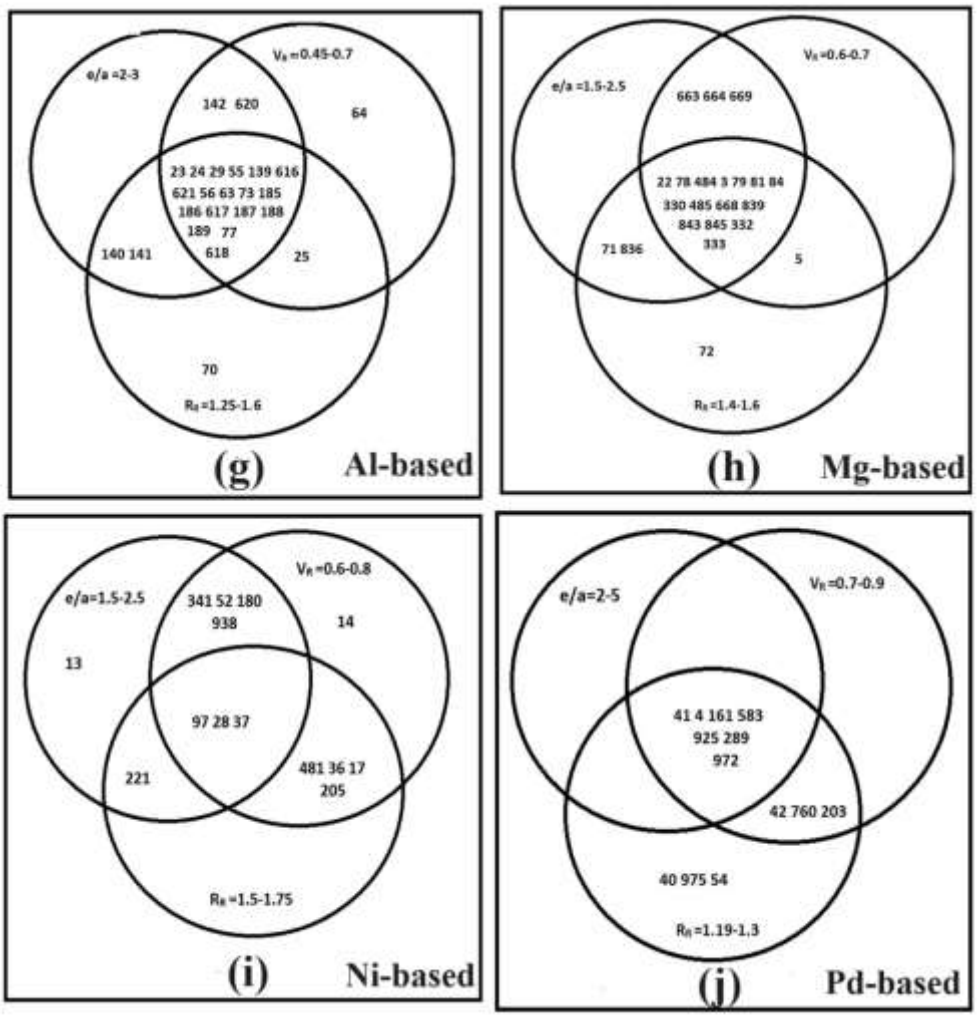

Fig. 2. 4: Venn diagram model for (g) Al-based system, (h) Mg-based system, (i) Ni-based system and (j) Pd-based system.

Table 2. 4: Number of systems following glass forming criteria in the range given in columns 5 to 7

System	e/a criteria	V_R criteria	R_R criteria	e/a range	V_R range	R_R range
Cu	28	31	30	1-2	0.5-0.75	1.25-1.5
Zr	31	31	31	1-2	0.7-0.85	1.25-1.51
Ti	40	35	37	2-3	0.65-0.85	1.25-1.45
La	15	11	15	1-2.5	0.7-0.8	1.4-1.55
Mg	20	19	19	1.5-2.5	0.6-0.7	1.4-1.6
Co	13	11	12	1-2	0.5-0.6	1.6-1.75
Al	22	22	22	2-3	0.45-0.7	1.25-1.6
Ni	9	12	8	1.5-2.5	0.6-0.8	1.5-1.75
Pd	7	10	13	2-5	0.7-0.9	1.2-1.3

It is due to the addition of semi-metallic or metalloids like Silicon, boron, phosphorus, and carbon addition. In non-ferrous-based metallic glasses, it is observed that to addition of transition metals enhances the GFA[4], [23], [28]. Further, such systems have very little (0.5 or 1 at. %) metalloid addition. All those non-ferrous BMGs conforming to the addition of transition metals and metalloids are lying in the intersection regions of the three criteria. Those alloy systems bearing numbers 40, 42, 54, 64, 191, 203, 760, 975, 988, and 989 are different in view of e/a values. These alloy systems have their e/a value of either 0.64 or 5.04 from those of others as they are outside the range of the three computed parameters given in tables as well as in the Venn diagrams. Also, alloy systems designated by numbers 40, 42, 54, 141, 172, 216, 425, 426, and 908 possess V_R either 0.23 or 0.93 which are outside the range of V_R for other BMG compositions. It is observed that the V_R parameter seems to be very important and value-sensitive towards alloy compositions like that of e/a. Our computation reveals the importance of this parameter in GFA.

Table 2. 5: Number of alloy systems falling in the intersection regions of the Venn-diagrams

Major elements of alloy systems	e/a, V_R , R_R	e/a and V_R	e/a and V_R	V_R and R_R
Fe	49	6	13	2
Cu	25	1	2	3
Zr	27	1	2	2
Ti	30	3	5	2
La	11	Nil	4	Nil
Mg	15	3	2	1
Co	10	Nil	1	1
Al	18	2	2	1
Ni	3	4	1	4
Pd	7	Nil	Nil	3

2.5. Role of G1, G2, and K_F

In the preceding section, the GFA was assessed in terms of e/a, V_R, and R_R for various alloy systems. Now, it is my turn to comment on the stabilization of such compositions in terms of the interaction of PBZ and FS. For better continuity, the Fermi vector (K_F) as well as half the value of G_1 and G_2 are listed in ANNEXURE-I. G_1 and G_2 are reported only for those systems for which diffraction studies on the MGs/BMGs are carried out after controlled crystallization in the literature. For an understanding of the amorphous structure, one can assume that the diffuse diffracting boundary that has the most intense diffracting wall is situated at a reciprocal distance of $G_1/2(Å^{-1})$. This defines the radius of pseudo- Brillouin zone surface. Fermi vector K_F indicates the radius of the spherical Fermi surface.

It has been observed that all MGs display diffuse intensity maxima around d values corresponding to the intermetallic phases formed in a similar composition on controlled crystallization of MGs. The values of $G_1/2$ for all MGs/BMGs are given in ANNEXURE-I with relevant references. I take only thirteen values. These are 1.09, 1.12, 1.22, 1.26, 1.33, 1.39, and 1.46, 1.53 and $1.59Å^{-1}$ correspond to the location of the first diffuse intensity maxima. Very few systems take the values of 1.31 and 1.86 $Å^{-1}$ and others take 1.46 and $2.37A^{o-1}$. It is worth noting that note that compositions of MGs/BMGs falling in the intersection region of all three criteria have almost

equal values of $G_1/2$ in their respective systems. All the values of $G_1/2$ and $G_2/2$ are listed in tables which I provided in ANNEXURE-I along with relevant references. After analysis of XRD patterns of both BMGs and their crystalline phase, it is important to point out here that the resulting crystalline or quasi-crystalline phases have first intense intensity maxima that is G_2 appearing around G_1. This phenomenon depends on the compositions of MGs/BMGs. This indicates the inheritance of common clusters in the crystalline/quasi-crystalline and glassy phases[20]. Further, it was observed that long-range translational solids in crystalline/quasi-crystalline states have characteristics of complex intermetallic. These complex intermetallic have large unit cell volumes [135] and clusters of atoms at each of the lattice points in the crystalline state. This is an important feature for MGs/BMGs formation which indicate there are limited class of clusters which promote glass formation. According to Kelton et al.[20], those BMG alloys have large unit cell volumes and bigger size of clusters vis-à-vis has lesser degree of fragility. In this sense, fragility and larger size clusters in the liquid state appear to be coupled. Nagel et al.[126], experimentally observed that mono-valent elements have Fermi radius (K_F) < $G_2/2$ and divalent elements have $K_F > G_2/2$. For a multi-component system, the glass compositions which have $K_F \approx G_1/2$ their e/a ratio are lying between 1 and 2. Such systems are stable and it is only due to the interaction of FS and PBZ interaction. It was observed that Fermi-surface and Brillouin-zone interaction takes place for those systems for which $K_F \approx G_1/2$[22][30]. All the MGs/BMGs systems that fulfil the above condition are listed in Table 11 in Annexure 1. One note from this, all these alloy systems have an e/a ratio lying between 1 and 2. These MGs/BMG systems are a class in themselves. Such a system is stabilized by the interaction of the Ferni-surface and Brillouin zone. However, many other MGs/BMGs also have their e/a value between 1 and 2 but such an interaction does not exist. Their stability can be understood differently. This will not be investigated here.

Based on diffraction evidence from all the 303 representative alloy systems among ~1000 MGs/BMGs compositions whose diffraction studies are available in the literature contain essentially nine different types of intermetallic phases. These intermetallic phases with space groups belong to I-4(Ni3P), Fddd (Mg2Cu), Fm-3m(Cr234C6), I4/mmm (Ti3Cu4), Fd-3m(MgCu2), P62m(Fe2P), I4/mcm (Al2Cu), and Ab2a(Zr7Ni10). The symbols in parentheses represent the Pearson symbols for these structures. Table 6 gives the structure of these intermetallic phases that fulfil the above criteria.

Table 2. 6: Crystallographic details of phases after devitrification or crystallization of BMGs

Experimental d(Å)	G2/2	System	Phase present/plane/ lattice parameter(Å)	Structure type/ space group (s.g. no.)	Remark and references
1.98	1.58	151	Tetragonal/(a=9.1, c=4.465)	Ni3P/ I-4	tI32[136]
2.03	1.54	79	Orthorhombic/ (224)/ (a=5.26, b=9.02, c=18.31)	Mg2Cu/ Fddd	oF48[137]
2.07	1.51	247, 696, 308, 978, 172	FCC/(511)/(a=10.76)	Cr23C6/Fm-3m	cF116[138]
2.08	1.51	20	Icosahedral	Pm35	[139]
2.1	1.49	506, 507	Tetragonal/ (107)/ (a=3.13, c=19.94)	Ti3Cu4/I4/mmm	tI14[140]
2.12	1.48	485	FCC/ (311)/ (a=7.03)	MgCu2/ Fd-3m	cF24[141]
2.13	1.47	40	Hexagonal/ (420)/ (a=13.055, c=27.49)	Fe2P/ P62m	hP288[138]
2.18	1.44	10	FCC/(511)/(a=11.32)	Ti2Ni/ Fd-3m	cF96[142]
2.24	1.4	52	Orthorhombic/ (422)/ (a=12.38, b=9.15, c=9.21)	Zr7Ni10/ C2Ca	oC68[143]
2.28	1.37	985	Orthorhombic/ (a=12.67, b=9.3, c=9.35)	Zr7Ni10/Ab2a	oC68[144]
2.34	1.34	9	Icosahedral	Pm35	[145]
2.54	1.23	940,941	Tetragonal/ (a=6.385, c=5.59)	Al2Cu/ I4/mcm	tI12[146]

From Table 2.6, it can be clearly observed that the intermetallic that are formed in MGs/BMGs have bearing with unique crystal structures. These crystal structures are cubic, tetragonal, orthorhombic, and hexagonal phases.

2.6. Alloy Compositions Selection

There are a huge number of MGs/BMGs compositions based on different systems present in the literature but my interest is in Fe-based metallic glass formation for structural applications only. Fe-based MGs/BMGs known as amorphous steels are stronger, stiffer, harder, lighter, highly corrosion resistant, and non-magnetic or soft-magnetic in nature as compared to some other novel and advanced materials[4]. Based on the work of Azad et al.[128] and Kumari and Mandal[147], I have chosen four BMG compositions from the literature for experimental investigations.

For the formation of Fe-based MGs/BMGs, the e/a ratio is to lie in the range of 1-2, the V_R values in the range of 0.5-0.9, and R_R in the range of 1.5-2. Keeping these in view four compositions are selected here. The details of nominal compositions are given in Table 2.7.

Table 2. 7: Selected Compositions with various glass-forming parameters (based on Venn diagram model)

Compositions designation	Selected Compositions (at %)	e/a	V_R	R_R
A	$Fe_{61}Cr_4Mo_{14}C_{15}B_6$[148]	2.17	0.66	1.61
B	$Fe_{48}Cr_{15}Mo_{14}C_{15}B_6Y_2$ [120], [121]	1.67	0.47	2.33
C	$Fe_{45}Cr_{20}Mo_{10}W_2C_{15}B_6Y_2$ [122]	1.33	0.11	2.33
D	$Fe_{45}Cr_{15}Mo_{14}Co_3C_{15}B_6Y_2$ [123]	1.74	0.12	2.33

The above compositions were prepared by different processing routes by different researchers. Gu et al.[148], successfully synthesized $Fe_{61}Cr_4Mo_{14}C_{15}B_6$ BMG of 2 mm rod in Suction-casting into Cu-mould casting. Iqbal et al.[120] and Lu et al.[121], synthesized $Fe_{48}Cr_{15}Mo_{14}C_{15}B_6Y_2$ BMG of 4 mm diameter rod by using injection in-to Cu-mould and induction melting followed by Cu-mould casting respectively. Liang et al.[122], successfully produced a 6 mm diameter BMG of composition $Fe_{45}Cr_{20}Mo_{10}W_2C_{15}B_6Y_2$ by using drop casting into Cu-mould technique. They also produce amorphous ribbons of 1.2 mm width and ~ 40μm thick. Qing-Jun et al.[123], produce 8mm diameter rod of $Fe_{45}Cr_{15}Mo_{14}Co_3C_{15}B_6Y_2$ BMG by using arc-melting followed by Cu-mould casting technique. It has been noted that with the small addition of alloying elements and by changing the processing technique, the possibility of glass formation is investigated. This will be the major part of the studies reported in subsequent chapters.

2.7. Conclusions

Based on the Venn diagram model, I have successfully categorized 303 representative alloy systems among ~ 1000 BMG compositions. The Venn diagram model is based on three following glass-forming parameters e/a, V_R, and R_R. Among three the e/a and V_R are very important compositional dependent glass-forming parameters. The range of e/a for different system-based alloys are given below:

(i) Fe-, Cu-, Zr-, and Co-based system lies between 1 and 2

(ii) Ti-, and Al-based system between 2 and 3

(iii) La-based system between 1 and 2.5

(iv) Mg-based system between 1.5 to 2.5

(v) Pd-based system between 2 and 5

It was seen that the majority of alloy systems have e/a lying between 1 and 2. Such alloys have further been classified into two categories. The first category of alloy system displays the Fermi-surface and the Pseudo-Billouin zone intersection. In other category does not have such an interaction. The former is understood in literature but the latter has not been attempted so far. Hence this will not be deliberated further.

Based on empirical correlation, I have selected four Fe-based glass-forming compositions. The effect on structures/microstructures under various processing conditions (cf. Chapter 4,5,6) will be investigated. A detailed indentation behavior of the samples will also be studied to assess their hardness characteristics for comparison with maraging steel as well as those reported for amorphous steel.